ISSN 1674-1056
http://cpb.iphy.ac.cn
http://iopscience.iop.org/cpb
中国物理 B
Chinese Physics
中国物理 Chinese Physics B

1.3-μm InAs/GaAs quantum dots grown on Si substrates

Fu-Hui Shao(邵福会), Yi Zhang(张一), Xiang-Bin Su(苏向斌), Sheng-Wen Xie(谢圣文), Jin-Ming Shang(尚金铭), Yun-Hao Zhao(赵云昊), Chen-Yuan Cai(蔡晨元), Ren-Chao Che(车仁超), Ying-Qiang Xu(徐应强), Hai-Qiao Ni(倪海桥), Zhi-Chuan Niu(牛智川)

Citation: Chin. Phys. B . 2018, 27(12): 128105. **doi:** 10.1088/1674-1056/27/12/128105
Journal homepage: http://cpb.iphy.ac.cn; http://iopscience.iop.org/cpb

What follows is a list of articles you may be interested in

Facilitative effect of graphene quantum dots in MoS_2 growth process by chemical vapor deposition

Lu Zhang(张璐), Yongsheng Wang(王永生), Yanfang Dong(董艳芳), Xuan Zhao(赵宣), Chen Fu(付晨), Dawei He(何大伟)
Chin. Phys. B . 2018, 27(1): 018101. **doi:** 10.1088/1674-1056/27/1/018101

Electric-field-dependent charge delocalization from dopant atoms in silicon junctionless nanowire transistor

Hao Wang(王昊), Wei-Hua Han(韩伟华), Xiao-Song Zhao(赵晓松), Wang Zhang(张望), Qi-Feng Lyu(吕奇峰), Liu-Hong Ma(马刘红), Fu-Hua Yang(杨富华)
Chin. Phys. B . 2016, 25(10): 108102. **doi:** 10.1088/1674-1056/25/10/108102

Synthesis of ZnO quantum dots and their agglomeration mechanisms along with emission spectra based on ageing time and temperature

Bo Qiao(乔泊), Suling Zhao(赵谡玲), Zheng Xu(徐征), Xurong Xu(徐叙瑢)
Chin. Phys. B . 2016, 25(9): 098102. **doi:** 10.1088/1674-1056/25/9/098102

Bound states of Dirac fermions in monolayer gapped graphene in the presence of local perturbations

Mohsen Yarmohammadi, Malek Zareyan
Chin. Phys. B . 2016, 25(6): 068105. **doi:** 10.1088/1674-1056/25/6/068105

Defect reduction in GaAs/Si film with InAs quantum-dot dislocation filter grown by metalorganic chemical vapor deposition

Wang Jun, Hu Hai-Yang, Deng Can, He Yun-Rui, Wang Qi, Duan Xiao-Feng, Huang Yong-Qing, Ren Xiao-Min
Chin. Phys. B . 2015, 24(2): 028101. **doi:** 10.1088/1674-1056/24/2/028101

1.3-μm InAs/GaAs quantum dots grown on Si substrates*

Fu-Hui Shao(邵福会)[1,2], Yi Zhang(张一)[1,2], Xiang-Bin Su(苏向斌)[1,2], Sheng-Wen Xie(谢圣文)[1,2], Jin-Ming Shang(尚金铭)[1,2], Yun-Hao Zhao(赵云昊)[3], Chen-Yuan Cai(蔡晨元)[3], Ren-Chao Che(车仁超)[3], Ying-Qiang Xu(徐应强)[1,2], Hai-Qiao Ni(倪海桥)[1,2], and Zhi-Chuan Niu(牛智川)[1,2,†]

[1] *State Key Laboratory for Superlattices and Microstructures, Institute of Semiconductors, Chinese Academy of Sciences, Beijing* 100083, *China*
[2] *College of Materials Science and Opto-Electronic Technology, University of Chinese Academy of Sciences, Beijing* 100083, *China*
[3] *Laboratory of Advanced Materials, Department of Materials Science, Collaborative Innovation Center of Chemistry for Energy Materials (iChEM), Fudan University, Shanghai* 200433, *China*

(Received 14 August 2018; revised manuscript received 26 September 2018; published online 10 November 2018)

We compare the effect of InGaAs/GaAs strained-layer superlattice (SLS) with that of GaAs thick buffer layer (TBL) serving as a dislocation filter layer. The InGaAs/GaAs SLS is found to be more effective than GaAs TBL in blocking the propagation of threading dislocations, which are generated at the interface between the GaAs buffer layer and the Si substrate. Through testing and analysis, we conclude that the weaker photoluminescence for quantum dots (QDs) on Si substrate is caused by the quality of capping $In_{0.15}Ga_{0.85}As$ and upper GaAs. We also find that the periodic misfits at the interface are related to the initial stress release of GaAs islands, which guarantees that the upper layers are stress-free.

Keywords: quantum dots, dislocation filter, molecular beam epitaxy (MBE), silicon photonics

PACS: 81.15.Hi, 81.07.Ta, 83.85.St, 85.35.Be **DOI:** 10.1088/1674-1056/27/12/128105

1. Introduction

Si-based optical materials and devices have been extensively investigated in the last few years[1–6] because Si-based laser was considered to be the holy grail of Si photonics for the researchers of photonic communities. However, Si is an indirect bandgap material and the radiative recombination process for an Si emitter is insignificant compared with nonradiative recombination process. Direct bandgap III–V compounds have robust photonic properties for semiconductor emitters in a wide range of photonic applications.[7,8] Therefore, heteroepitaxial growth of III–V compound semiconductor materials on Si is one of the most promising ways to realize Si-based laser fabrication. The difficulties in monolithically integrating the GaAs on Si substrates consist in the differences in lattice constant and thermal expansion coefficient among them, and the formation of anti-phase domains (APDs) due to the polar/nonpolar interface of III–V/IV.[9] The high-density threading dislocations (TDs) are generated by misfit of lattice constant and misfit of thermal expansion coefficient, and could propagate into the active region and become nonradioactive recombination centers, and hence lead to significant degeneration of the optoelectronic conversion efficiency and device lifetime.[10,11]

Studies have shown that using (100) oriented Si substrates with 4° offcut toward [110] plane could reduce the formation of APDs,[12] besides, a pre-layer technique could also lessen the APDs. As for the elimination of TDs, some means have been used, like substrate graphic processing,[13] transition buffer layer growth, materials like Ge or GaP,[14–16] whose lattice constant is in the middle of Si's and GaAs' lattice constant, introducing a thick GaAs buffer layer and strained-layer superlattices (SLS),[17–19] bonding,[20,21] *etc*. Although progress has been made in the hetero-epitaxial growth of III–V compound on Si, the research in this field, on the whole, is not in-depth and many issues remain to be further investigated.

In the case of direct growth of GaAs on Si, thick GaAs buffer layer (TBL) and SLS are desirable,[22,23] because they are not as complicated as the alternatives and they do not introduce additional processes. The InGaAs/GaAs strained-layer superlattices could reduce the dislocation density because the strain of SLS can filter out TDs.[17,24] Research of the thick buffer layer has shown that the TDs decrease with the increase of GaAs thickness.[25] However, most of the previous studies focused on the structure and growth condition of SLS and buffer layer.[17–19,24] The efficiencies of these two methods in eliminating the TDs and the comparison between their active region quality have not yet been reported. Since the photoluminescent wavelength of InGaAs/GaAs quantum dot (QD) is in the range of communication band, we grow the InGaAs/GaAs QDs on the top of SLS and TBL serving as the active layers. In addition, the measurement of QD luminescent property is an extremely convincing way to test the crys-

*Project supported by the National Key Research and Development Program of China (Grant No. 2018YFA0306101), the Scientific Instrument Developing Project of Chinese Academy of Sciences (Grant No. YJKYYQ20170032), and the National Natural Science Foundation of China (Grant Nos. 61790581, 61435012, and 61505196).

†Corresponding author. E-mail: zcniu@semi.ac.cn

© 2018 Chinese Physical Society and IOP Publishing Ltd

tal quality of the entire epitaxial material. In this paper, we find that the periodic misfits in the interface are related to the initial stress release of GaAs islands, which guarantees that the upper layers are stress-free. We also demonstrate that the SLS is more effective in blocking the TDs than GaAs thick buffer layer because its stress could suppress the misfits from reacting to each other. Therefore, the photoluminescence (PL) of QDs grown on the SLS buffer layer has a better quality than on the GaAs TBL.

2. Experimental details

To suppress the APDs, all the Si substrates were in the (100) direction with 2°–4° offcut towards the [110] plane. The oxide desorption was performed by holding the Si substrates at a temperature of 1100 °C for 20 min. The RHEED image shows a clear (2 × 1) reconstruction of Si, which indicates the surface is clear and the formation of double monolayer steps.[26] The substrate was then cooled down to 380 °C for growing a 5-nm AlAs as the nucleation layers and a 30-nm GaAs followed as the low temperature buffer layer (LTBL). Its growth rate was the same as the AlAs nucleation layer's, as low as 0.1 monolayer (ML)/s. The temperature then increased up to 480 °C, a 100-nm middle temperature buffer layer (MTBL) was grown with a growth rate of 0.3 ML/s, followed by annealing at 650 °C for 5 min. Then, an additional 870-nm high temperature buffer layer (HTBL) was grown with a growth rate as high as 0.58 ML/s at 580 °C.

For sample A, another set of LTBLs, MTBLs, and HTBLs were grown on the as-grown structure. For sample B, three repeats of SLS and 400-nm GaAs were deposited on the as-grown structure. The growth of SLS included a five-period (10-nm-$In_{0.15}Ga_{0.85}As$/10-nm GaAs) superlattices at 420 °C on the as-grown structure, followed by annealing at 610 °C for 5 min, which can further strengthen the effect of SLS in reducing the TDs.[24] Then the substrate temperature decreased down to 580 °C for growing the 400-nm GaAs. Sample C was grown on the exact GaAs (100) substrate, and the QDs were also grown on the top of 300-nm GaAs buffer layer used for the contrast experiment.

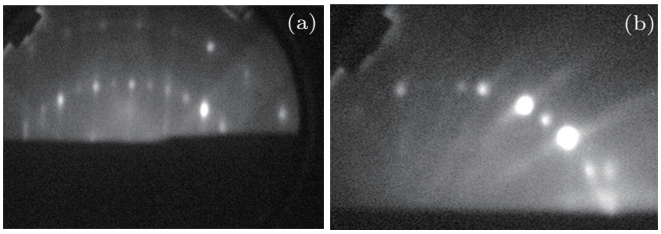


Fig. 1. RHEED image of clear Si surface. (a) (2 × 1) reconstruction of [100] direction and (b) (2 × 1) reconstruction of [110] direction.

The growth parameters of QDs for all samples are identical, a five-layer InAs/GaAs quantum dot (QD) was grown on the top of the structure, which consists of 2.5-ML InAs at the bottom, 5-nm $In_{0.15}Ga_{0.85}As$ in the middle and 40-nm GaAs on the top. Only the top QD layer was uncapped for the Atomic Force Microscopy (AFM) measurement. The PL test was also carried out on the surface of uncapped QDs. All of the materials were grown in a Veeco Gen 930 MBE system, and the different structures of all samples are shown in Fig. 2.

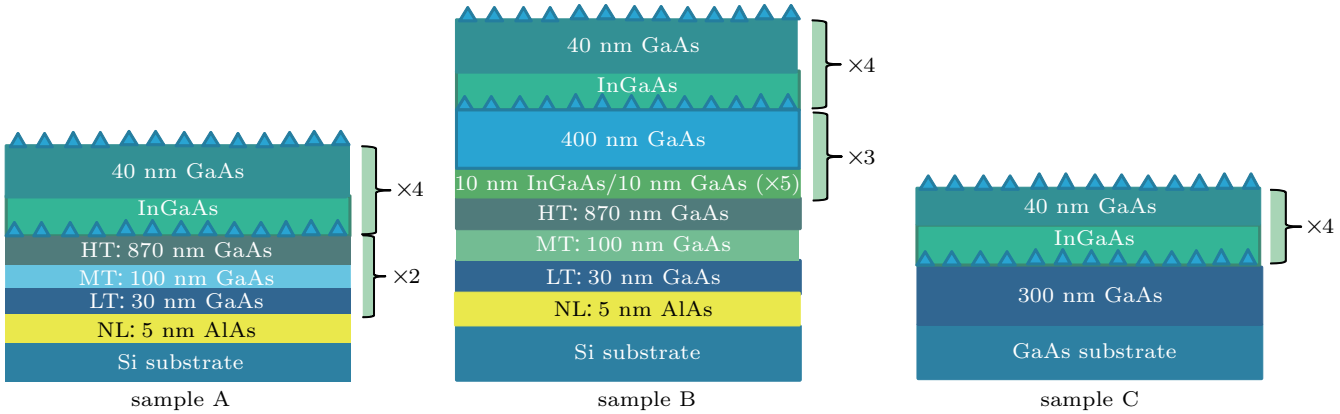


Fig. 2. (color online) Schematics of InAs/GaAs QDs on Si and GaAs substrates.

3. Results and discussion

The measurement of PL spectrum and AFM are shown in Fig. 3. The intensity of sample A is half the intensity of the GaAs substrate and one-sixth the intensity of sample B. The full width at half maximum (FWHM) is 58 meV for sample A and 61 meV for sample B compared with the 35 meV for GaAs. Figure 4 shows the cross-sectional TEM view of the as-grown structure on an Si substrate. The high densities of threading dislocations are visible in both samples. While the GaAs TBL and SLS could stop most of the TDs from propagating into the active region, there are still some dislocations penetrating into the QDs region and reducing the PL. And it is the reason why their PL intensity and FWHM are worse than QDs grown on a GaAs substrate. To understand how the TDs

affect the active region, we study the surface appearance by combining the SEM testing method.

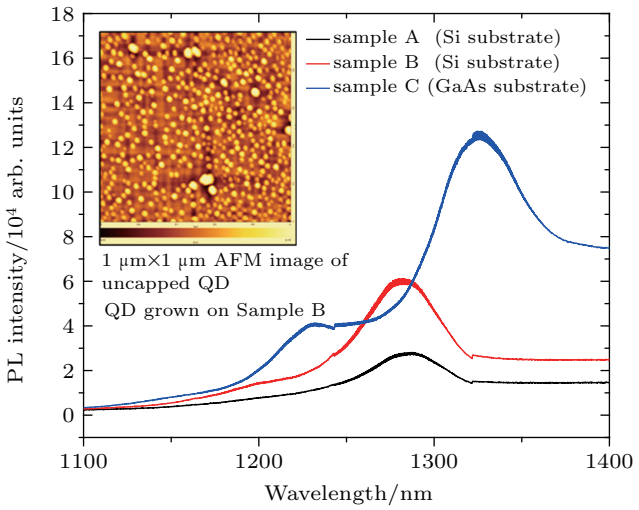


Fig. 3. (color online) Room-temperature PL spectra and AFM image of InAs/GaAs QDs sample.

The density of QDs is about 10^{10} cm^{-2}–10^{11} cm^{-2}, and studies show that the density of TDs that could propagate into the active region for samples A and B are both about 10^4 cm^{-2}–10^7 cm^{-2},[24] according to

$$\rho_{\mathrm{TD}} = \frac{\rho_{\mathrm{TD}}^{(0)}}{1 + 2Rq\tan(\theta)\rho_{\mathrm{TD}}^{(0)}h}, \tag{1}$$

which is proposed by Romanov, it is the most general TBL calculation equation. In Eq. (1),[27] θ is the angle between line direction of TDs and perpendicular direction, h is the layer thickness; R is the capture radius: if the distance between dislocations is less than R, it is deemed that the dislocations meet and react with each other because of the energetically favorable reaction; q is the possibility of annihilation of one of the TDs in each encounter; $\rho_{\mathrm{TD}}^{(0)}$ is the initial TD density at $h = 0$. For sample B, the relationship between the strain and density of TDs is

$$\rho_{\mathrm{TD}}(\varepsilon_{\mathrm{r}}) = \rho_{\mathrm{TD}}^{(0)} \exp\left(\frac{-2Rq\varepsilon_{\mathrm{r}}}{Db_{\parallel}}\right), \tag{2}$$

where D is a constant relating to the array; $b_{\parallel}$ is the magnitude of the Burgers vector component that relieves misfit strain; ε_{r} is the strain of material, and the relaxation of it can be produced by TDs' moving.[28]

The size of one QD is about a dozen of nanometers, so in one square centimeter, only few hundredths of the area is take up by QDs. Combining with the SEM test in Fig. 5, it is shown that no TDs along the surface react with a raw of QDs. We can conclude that most of the TDs have a small angle relative to the surface normal; that is, there is no TD alongside the surface. So we can assume that the possibility for a TD to directly pass though a quantum dot is too small to affect the PL intensity. Although the TDs do not greatly affect the QDs, they have a dramatic influence on the quality of capping $In_{0.15}Ga_{0.85}As$ and upper GaAs. The TDs could become the non-radiative recombination centers in the energy gap and trap some of carriers, which explains why the PL intensity of QDs on Si is lower than on GaAs substrate. In this paper, we demonstrate that the SLS is more efficient in blocking the TDs than the TBL, and the capping $In_{0.15}Ga_{0.85}As$ and the upper GaAs lead to weak PL.

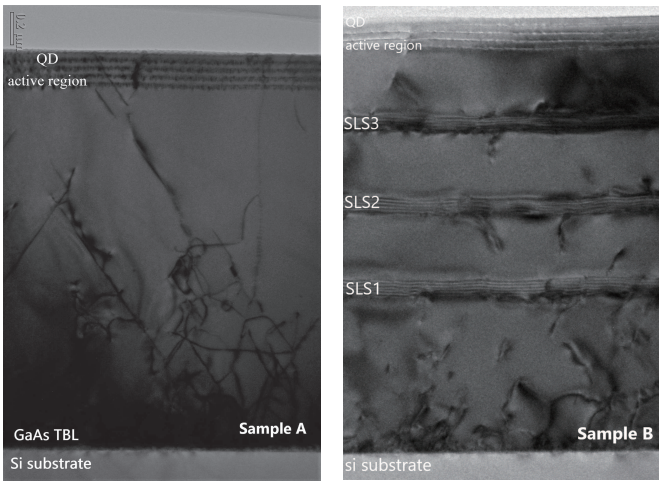


Fig. 4. Cross-sectional TEM image of InAs/GaAs QD on Si substrate.

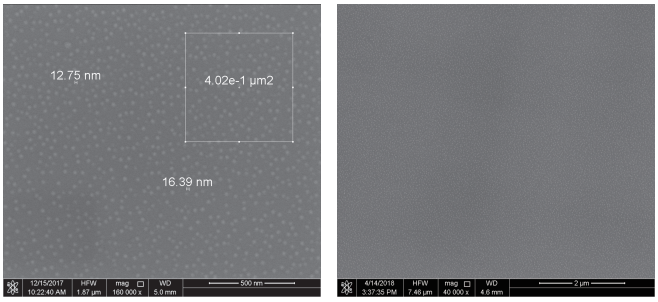


Fig. 5. SEM surface analysis of sample B.

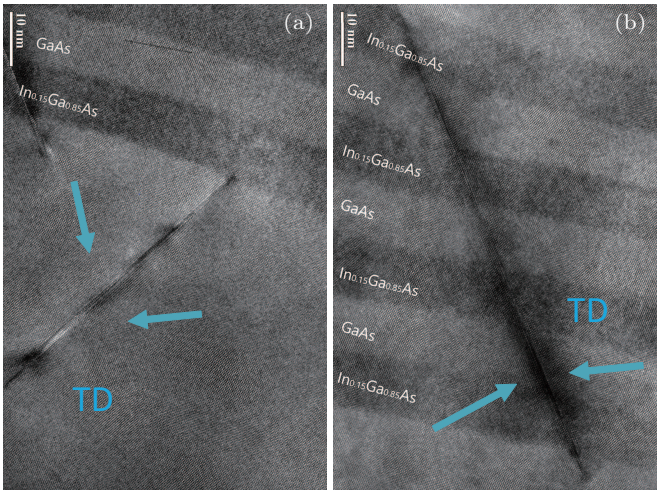


Fig. 6. (color online) TEM images of SLS reacting with TD: (a) SLS blocking the TDs and (b) TD penetrating into active region.

Figure 4 shows that the PL intensity of sample B with SLS is three times as high as that of sample A; that is, the strain of $In_{0.15}Ga_{0.85}As$/GaAs suppresses the TDs. Under the effect of strain, some orientation TDs react with each other. If they conform with the lowest energy principle, then the defects will disappear as shown in Fig. 6(a). But in sample B there are still some TDs that have penetrated into the active region as shown in Fig. 6(b), thus degenerating the material quality of surrounding $In_{0.15}Ga_{0.85}As$ and GaAs. But the number of TDs penetrating into active region of sample B is less than that of sample A; that is, the SLS is more efficient in blocking TDs than the TBL. So the PL intensity of sample B is much stronger than that of sample A.

To further understand the defects and their micron-stain, we use the geometric phase analysis (GPA)[29] to analyze the interface between GaAs and Si, and the QDs. The core principle of GPA is that by Fourier transforming the high resolution image of TEM, microscopic stress can be analyzed. Phase and displacement are related by

$$P_g(r) = -2\pi g \cdot u(r). \tag{3}$$

And the 2D displacement and phase are related with

$$u(r) = -\frac{1}{2\pi}\left[P_{g1}(r)a_1 + P_{g2}(r)a_2\right], \tag{4}$$

$$g_i \cdot a_j = \delta_{ij}. \tag{5}$$

So the phase gradient and reciprocal lattice deviation are related by

$$\nabla P_g(r) = 2\pi \Delta g(r). \tag{6}$$

Then

$$\varepsilon_{ij} = \frac{1}{2}\left(\frac{\partial u_i}{\partial x_j} + \frac{\partial u_j}{\partial x_i}\right), \quad i.e.,$$

$$\varepsilon_{xx} = \frac{\partial u_x}{\partial x}, \quad \varepsilon_{yy} = \frac{\partial u_y}{\partial y}, \quad \varepsilon_{xy} = \frac{1}{2}\left(\frac{\partial u_x}{\partial y} + \frac{\partial u_y}{\partial x}\right), \tag{7}$$

$$\Delta_{xy} = \frac{1}{2}\left(\frac{\partial u_i}{\partial x_j} + \frac{\partial u_j}{\partial x_i}\right), \quad i.e., \quad \Delta_{xy} = \frac{1}{2}(\varepsilon_{xx} + \varepsilon_{yy}), \tag{8}$$

$$\omega_{ij} = \frac{1}{2}\left(\frac{\partial u_j}{\partial x_i} - \frac{\partial u_i}{\partial x_j}\right), \quad i.e., \quad \omega_{xy} = \frac{1}{2}\left(\frac{\partial u_y}{\partial x} - \frac{\partial u_x}{\partial y}\right). \tag{9}$$

The ε_{xx}, ε_{yy}, and ε_{xy} represent the strain of X direction, Y direction, and XY plane, respectively, and Δ_{xy} and ω_{xy} represent the mean dilatation and rotation in XY plane. These relations are only valid for small deformations; however, the GPA uses the full relations suitable for large deformations. Based on this, the GPA is made for the microscopic property measurement of material, so the distribution of the micron-stain and defects could be measured by this method. Figures 7 and 8 are the GPA results of Si hetero-epitaxy interface and InAs quantum dots, respectively.

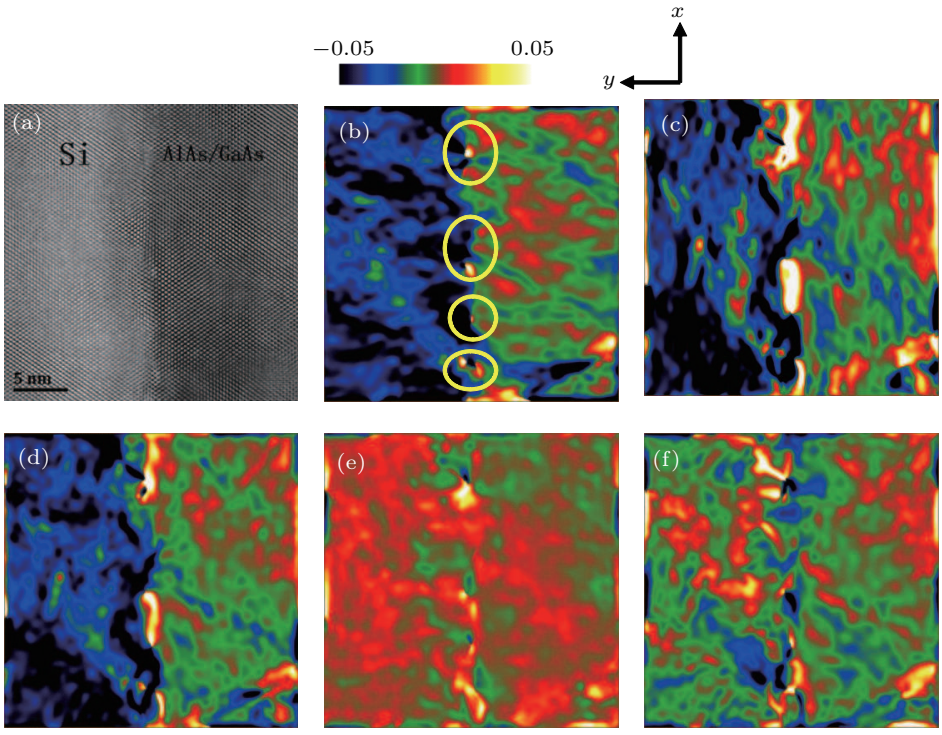


Fig. 7. (color online) GPA analysis of interface between Si and AlAs on sample A: (a) the interface of Si and AlAs, (b) ε_{xx}, (c) ε_{yy}, (d) Δ_{xy}, (e) ω_{xy}, and (f) ε_{xy}.

As shown in Figs. 7(b) and 7(c), the Si is displayed in blue and AlAs/GaAs is displayed in red, indicating that the lattice constant of Si substrate is smaller than that of GaAs and AlAs. The extreme value of ε_{xx} and ε_{yy}, marked by yellow circles, suggest that in these regions there are plenty of defects, including two types of defects; *i.e.*, I-type (Lomer misfits) and

II–type (60° misfits).[30] We find the extreme value periodically along the interface in both samples, and the period is about 5 nm–10 nm. It could be explained by the growth process of GaAs on Si. The initial GaAs islands are coherent with Si substrate, but with the increase of GaAs island, mismatch between Si and GaAs begins to show and lead to stress accumulation. When the size of GaAs island is big enough, the stress would be released and plenty of misfits appear at the interface. The period of misfit along the interface is related to the initial density of GaAs islands.[31–34]

The formation of periodic misfits guarantees that the thin film and active region are stain-free, as shown in Fig. 8. Although the color of InAs QDs's region is lighter than those in other parts, no extreme point is shown in GPA image, which means that QDs are defect free. If there is a TD crossing the QD, then the strain will abruptly change and extreme point will be shown in the GPA image. This can prove that the experimental results are consistent with the assumption as mentioned before that the possibility for a TD to directly cross a quantum dot is too small to impair the QDs quality. The QDs's GPA image for samples A and B are identical, so we can also conclude that the active region is strain-free for both samples. The initial growth of buffer GaAs layer makes the upper layers stain-free, because the initial misfits between GaAs and Si release the mismatch stress.

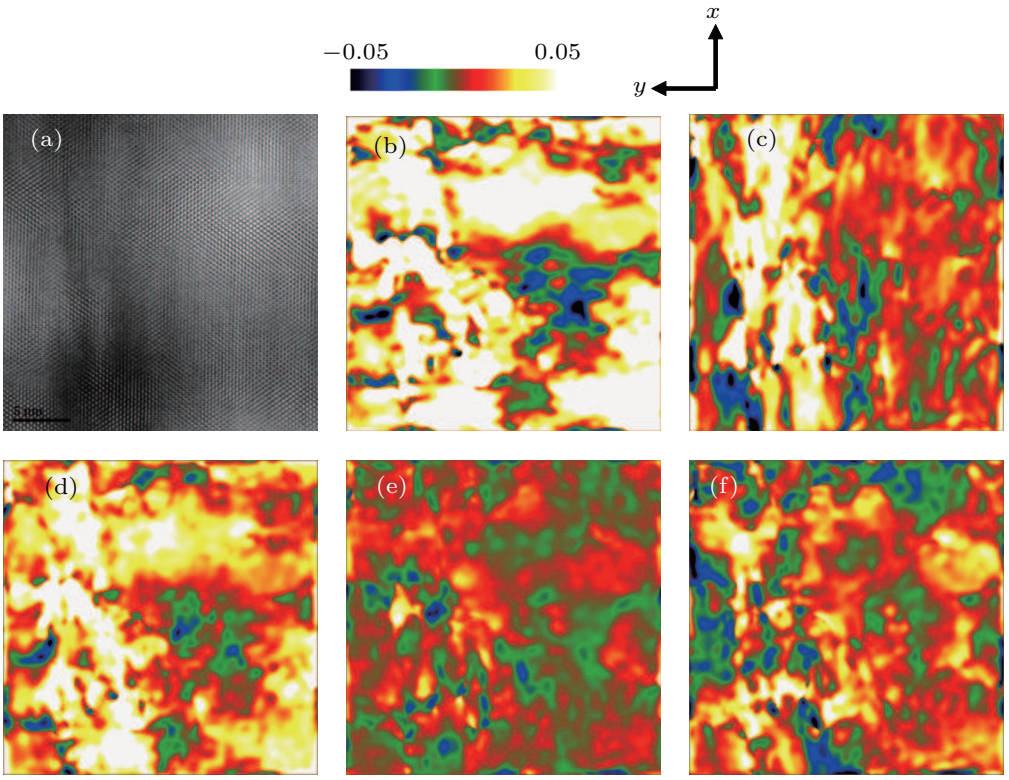


Fig. 8. (color online) GPA analysis of stress free InAs quantum dots: (a) the quantum dot of InAs, (b) ε_{xx}, (c) ε_{yy}, (d) Δ_{xy}, (e) ω_{xy}, and (f) ε_{xy}.

4. Conclusion

We introduce two methods of growing QDs on Si substrates, and the QDs' density is as high as the GaAs substrate's; *i.e.*, about 10^{10} cm^{-2} $\sim$ 10^{11} cm^{-2}. From the measurements of SEM and GPA, we conclude that the initial misfits could release the stress caused by lattice constant mismatch. This mechanism guarantees that the active regions are stress-free. Although the quality of InAs QDs is the same for two samples, SLS shows better PL quality than TBL. The growth of SLS means that most of the TDs are blocked under the buffer layer and disappear by reacting with other TDs. Furthermore the quality of $In_{0.15}Ga_{0.85}As$ capping layer and upper GaAs layer are better than that of TBL. Finally, the FWHM of SLS is as low as 58 meV and intensity is one third of GaAs substrate.

Acknowledgment

The authors would like to thank Jing Zhang and Ye Yuan for experimental support, and also thank Jiang Wu, and Xiao-Ran Cui for their helpful discussion.

References

[1] Liang D and Bowers J E 2010 *Nat. Photon.* **4** 511
[2] Chen X, Li C and Tsang H K 2011 *Npg Asia Mater.* **3** 34
[3] Jalali B and Fathpour S 2007 *J. Lightwave Technol.* **24** 4600
[4] Park H, Fang A W, Cohen O, Jones R, Paniccia M J and Bowers J E 2007 *IEEE Photon. Technol. Lett.* **19** 230

[5] Chen Q, Yang J W, Osinsky A, Gangopadhyay S, Lim B and Anwar M Z, Asif K M, K D, Temkin H 1997 *Appl. Phys. Lett.* **70** 17

[6] Friesen M, Rugheimer P, Savage D E, Lagally M G, Weide D W, Joynt R and Eriksson M A 2002 *Phys. Rev. B* **67** 121301

[7] Su X B, Ding Y, Ma B, Zhang K L, Chen Z S, Li J L, Cui X R, Xu Y Q, Ni H Q and Niu Z C 2018 *Nanoscale Res. Lett.* **13** 59

[8] Wu J, Chen S, Seeds A and Liu H 2015 *J. Phys. D: Appl. Phys.* **48** 363001

[9] Fischer R, Masselink W T, Klem J, Henderson T, Mcglinn T C, Klein M V, Morkc H, Mazur J H and Washburn J 1985 *J. Appl. Phys.* **58** 374

[10] Balakrishnan G, Huang S, Dawson L R, Xin Y C, Conlin P and Huffaker D L 2005 *Appl. Phys. Lett.* **86** 3

[11] Kim Y H, Lee J Y, Noh Y G, Kim M D, Cho S M, Kwon Y J and Oh J E 2006 *Appl. Phys. Lett.* **88** 24

[12] Bringans R D, Biegelsen D K and Swartz L 1991 *Phys. Rev. B* **44** 3054

[13] Wan Y, Norman J, Li Q, Kennedy M J, Liang D, Zhang C, Huang D, Zhang Z, Liu A Y, Torres A, Jung D, Arthur C G, Hu E L, Lau K M and Bowers J E 2017 *Optica* **4** 940

[14] Chen S, Liao M, Tang M, Wu J, Martin M, Baron T, Seeds A and Liu H 2014 *Optoelectronics Lett.* **8** 20

[15] Liu H, Wang T, Jiang Q, Hogg R, Tutu F, Pozzi F and Seeds A 2011 *Nat. Photon.* **5** 416

[16] Lee A D, Jiang Q, Tang M, Zhang Y, Seeds A J and Liu H 2013 *IEEE J. Sel. Top. Quantum Electron.* **19** 1901107

[17] Chen S, Tang M, Wu J, Jiang Q, Dorogan V G, Benamara M, Mazur Y I, Salamo G J, Seeds A and Liu H 2014 *IEEE Semiconductor Laser Conference*, September 7–10, 2014, Mallorca, Spain, p. 240

[18] Tang M, Wu, J, Chen S and Jiang Q 2015 *IET Optoelectron.* **9** 61

[19] Liu A Y, Zhang C, Norman J, Snyder A, Lubyshev D, Fastenau J M, Liu A W K, Gossard A C and Bowers J E 2014 *Appl. Phys. Lett.* **104** 4

[20] Tanabe K, Guimard D, Bordel D, Iwamoto S and Arakawa Y T 2010 *Opt. Express* **18** 10604

[21] Guimard D, Tanabe K, Nomura M, Iwamoto S and Arakawa Y 2009 *Opt. Express* **17** 7036

[22] Bordel D, Guimard D, Tanabe K, Iwamoto S and Arakawa Y 2010 *Optics Express* **18** 10604

[23] Mi Z, Yang J, Bhattacharya P and Huffaker D L 2006 *Electron. Lett.* **42** 121

[24] Okamoto H, Watanabe Y, Kadota Y and Ohmachi Y 1987 *Jpn. J. Appl. Phys.* **26** 12

[25] George I, Becagli F, Liu H Y, Wu J, Tang M, Beanl and R 2015 *Semicond. Sci. Technol.* **30** 114004

[26] Aizaki N and Tatsumi T 1986 *Surf. Sci.* **174** 658

[27] Romanov A E, Pompe W, Beltz G and Speck J S 1996 *Phys. Status Solidi* **198** 599

[28] Ward T, Sánchez A M, Tang M, Wu J, Liu H, Dunstan, D J, Beanl and R 2014 *J. Appl. Phys.* **116** 6

[29] Chung J, Lian G and Rabenberg L 2010 *IEEE Electron Dev. Lett.* **31** 854

[30] Hÿtch M J, Snoeck E and Kilaas R 1998 *Ultramicroscopy* **74** 131

[31] Otsuka N, Choi C, Nakamura Y and Nagakura S 1986 *Appl. Phys. Lett.* **49** 277

[32] Wang T, Lee A, Tutu F, Seeds A, Liu H, Jiang Q, Groom K and Hogg R 2012 *Appl. Phys. Lett.* **100** 5

[33] Matthews J W 1975 *Epitaxial Growth* (New York: Elsevier Inc.) pp. 559–609

[34] Usui H, Yasuda H and Mori H 2006 *Appl. Phys. Lett.* **89** 173127